

PREPARED FOR THE U.S. DEPARTMENT OF ENERGY,
UNDER CONTRACT DE-AC02-76CH03073

PPPL-3663
UC-70

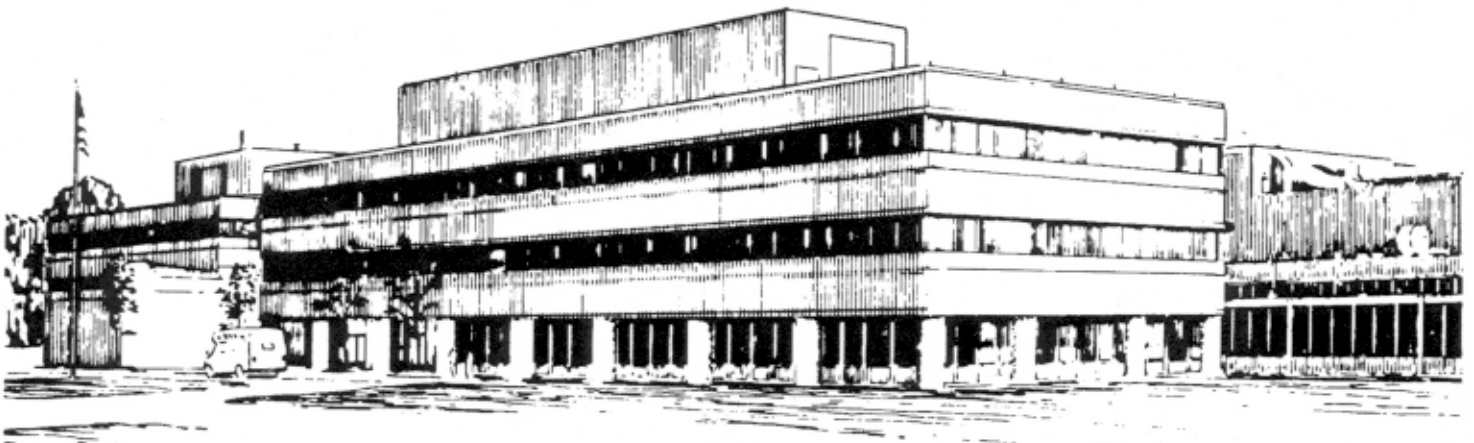
PPPL-3663

**Compressional Alfvén Eigenmode Dispersion
in Low Aspect Ratio Plasmas**

by

N.N. Gorelenkov, C.Z. Cheng, and E. Fredrickson

January 2002



**PRINCETON PLASMA PHYSICS LABORATORY
PRINCETON UNIVERSITY, PRINCETON, NEW JERSEY**

PPPL Reports Disclaimer

This report was prepared as an account of work sponsored by an agency of the United States Government. Neither the United States Government nor any agency thereof, nor any of their employees, makes any warranty, express or implied, or assumes any legal liability or responsibility for the accuracy, completeness, or usefulness of any information, apparatus, product, or process disclosed, or represents that its use would not infringe privately owned rights. Reference herein to any specific commercial product, process, or service by trade name, trademark, manufacturer, or otherwise, does not necessarily constitute or imply its endorsement, recommendation, or favoring by the United States Government or any agency thereof. The views and opinions of authors expressed herein do not necessarily state or reflect those of the United States Government or any agency thereof.

Availability

This report is posted on the U.S. Department of Energy's Princeton Plasma Physics Laboratory Publications and Reports web site in Fiscal Year 2002. The home page for PPPL Reports and Publications is: http://www.pppl.gov/pub_report/

DOE and DOE Contractors can obtain copies of this report from:

U.S. Department of Energy
Office of Scientific and Technical Information
DOE Technical Information Services (DTIS)
P.O. Box 62
Oak Ridge, TN 37831

Telephone: (865) 576-8401
Fax: (865) 576-5728
Email: reports@adonis.osti.gov

This report is available to the general public from:

National Technical Information Service
U.S. Department of Commerce
5285 Port Royal Road
Springfield, VA 22161

Telephone: 1-800-553-6847 or
(703) 605-6000
Fax: (703) 321-8547
Internet: <http://www.ntis.gov/ordering.htm>

Compressional Alfvén Eigenmode Dispersion in Low Aspect Ratio Plasmas. *

N. N. Gorelenkov, C. Z. Cheng, E. Fredrickson
Princeton Plasma Physics Laboratory, P.O. Box 451
Princeton, NJ, USA 08543-0451
e-mail: ngorelen@pppl.gov

21st January 2002

Abstract

Recent observations of new fast ion beam driven instabilities in MHz frequency range in National Spherical Torus experiments (NSTX) are suggested to be Compressional Alfvén Eigenmodes (CAEs). A new theory of CAEs applicable to low aspect ratio toroidal plasmas is developed based on the ballooning representation for the poloidal dependence of the perturbed quantities. In agreement with observations, the analytical theory predicts that CAEs are discrete modes with frequencies correlated with the characteristic Alfvén velocity of the plasma. Plasma equilibrium structure is essential to determine accurately the dispersion of CAEs. The mode structure is localized in both the minor radius and the poloidal directions on the low magnetic field side.

1 Introduction

Emissions in the ion cyclotron range of frequency driven by energetic particles have been observed in the past in tokamak experiments [1, 2, 3, 4]. It is believed to be the thermonuclear cyclotron instability of Compressional

*This work supported by DoE contract No. DE-AC02-76-CHO-3073.

Alfvén Eigenmodes (CAEs, also called fast Alfvén or magnetosonic eigenmodes) driven by products of thermonuclear reactions. In these tokamak experiments CAE instability has not produced significant effects on thermal plasma. One reason for the lack of CAEs effect on background ions is that the free energy available to destabilize CAEs is low because the fraction of energetic ions with velocity greater than the Alfvén velocity is very small in these tokamak experiments. However, in low aspect ratio spherical tokamaks (ST), such as National Spherical Torus experiment (NSTX) [5], the Alfvén speed is low in comparison with the injection velocity (at $\mathcal{E}_{b0} = 80keV$) of NBI ions, $v_{A0}/v_{b0} \simeq 1/4$. The NSTX is a low aspect ratio toroidal device with the ratio of the geometrical center major radius to minor radius, $R_{g0}/a = 0.85m/0.65m$. For NSTX the super-Alfvénic particle power available to sustain these modes is comparable with the total auxiliary heating power, much larger than that of fusion product fast ions in conventional tokamaks and thus much stronger CAE instabilities can be expected in NSTX. This seems to be true for all ST devices including a projected reactor size ST[6].

Recent NSTX observations of magnetic fluctuations measured by edge Mirnov coils show a broad and complicated frequency spectrum of coherent modes between $400kHz$ and up to $2.5MHz$, with the fundamental cyclotron frequency of background deuterium ions to be $f_{cD} = \omega_{cD}/2\pi = 2.3MHz$, calculated at the vacuum magnetic field at the geometrical axis of NSTX for $B_{g0} = 0.3T$ [7]. A very rich spectrum of modes are observed at the same time during the NBI injection. The mode frequencies correlate with the Alfvén velocity as the magnetic field and plasma density are varied. The mode excitation is sensitive to NBI injection angle. Particle losses were not seen during these instabilities.

There has been significant progress in the theory of CAEs in recent years. However, the majority of theoretical studies are based on the high aspect ratio approximation for toroidal plasma equilibria. In such a case the solution is weakly localized in poloidal direction (see Refs. [8][10][9] and references therein), and the toroidicity is considered as a perturbation to the cylindrical solution [11, 12]. Weak toroidicity theory predicts more poloidal localization as the aspect ratio decreases. Typically the eigenmode is localized between the turning points in the poloidal direction on the low field side of the plasma cross section and localized radially near the plasma edge. In addition, the ellipticity is also important in determining the VAE dispersion. Thus, a new theory for CAE structure and dispersion is required for STs.

Based on the measured fluctuation spectrum and their comparison with the results of our CAE model we interpret the observed phenomena as CAEs driven by energetic beam ions. Frequency spectrum of localized CAE solutions are discrete. It is primarily determined by the Alfvén frequency at the mode location and by the poloidal wavevector as $\omega_{CAE} = v_A m/r$, where m is the poloidal mode quantum number and r is the minor radius.

2 High frequency mode observations in NSTX

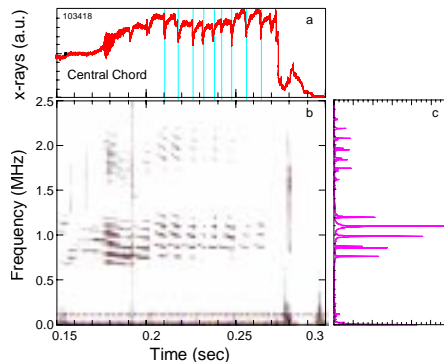


Figure 1: Time evolution of X-ray signal (a) and magnetic spectrum of high frequency modes (b) and one time slice of the spectrum taken at $t = 0.21sec$ (c) in NSTX shot #103418. NBI injection starts at $t = 0.15sec$

Coherent high frequency modes have been observed in NSTX with both high bandwidth magnetic pick-up coils and with reflectometers[7]. The range of operational parameters for the experiments discussed here are: toroidal current $I_p = 0.7 - 1MA$, toroidal field $B_{g0} = 3.0 - 4.5kG$, central electron density $n_{e0} = 1 - 5 \times 10^{19}m^{-3}$, central electron temperature of up to $T_{e0} = 1keV$. The plasmas are heated with a deuterium neutral beam injection (NBI) with power of $P_b = 1.5 - 3MW$. The data shown in Figure 1 reveal several common features of these modes. The modes appear about $\Delta t = 1 - 50msec$ after the start of neutral beam injection. In this example the mode frequencies decrease with time and the mode activities are terminated by the sawtooth crash. As shown in Fig. 1(c) the mode frequencies are approximately evenly spaced up to at least $2.5MHz$ (the full bandwidth of the system). The mode frequency spacing in this example is nearly uni-

form at about $\Delta f \simeq 120kHz$ and the spectral peaks appear in two bands spanning $0.7 - 1.2MHz$ and $1.5 - 2.2MHz$. These two bands are apparent in amplitude, and there are subtle variations in the similar spacing of the frequency peaks in each band. This suggests that these are distinct bands, e.g., with the frequency separation at $1.53MHz$. Each peak in Fig. 1(c) also consists of a bunch of subpeaks if shown with higher resolution. Such satellite subpeaks are separated by $\sim 20kHz$ from each other. Detailed measurements of the mode structure have not yet been done. However, initial data from the reflectometer, which measures the displacement of constant density contours, showed that the modes also produce density fluctuations in the plasma. The characteristic amplitude of the density oscillations deduced from the reflectometer measurements is about $\delta n_e/n_e \sim 1 - 3 \times 10^{-4}$.

Typically the bunches of frequency subpeaks follow the trend of $v_A \sim B/\sqrt{n_e}$, when the density and/or magnetic field were changed during the shot, where n_e is the characteristic electron density. Another common feature of these instabilities is the cutoff at low frequency, i.e. at $f = 500 - 700kHz$. More finer structure of the spectrum also shows that all unstable modes are bursting and damped simultaneously on a very short time scale. This behavior resembles the fishbone instability, except that in this case all modes behave similarly. The instability is very sensitive to the distribution function of NBI ion, which is determined by the injection angle and injection energy of NBI ions. However, it was observed that the frequency of high frequency unstable modes does not change due to the change in the NBI injection angle. One can conclude that CAEs are cavity modes determined by the thermal plasma properties. Typical magnitude of the perturbed magnetic field is small with $\delta B_{\parallel}/B \sim 2 \times 10^{-4}$ [7].

3 Strong toroidicity theory for CAEs in NSTX.

Estimates show [13] that the weak toroidicity theory fails to resolve with good accuracy the measured frequency spectra in NSTX experiments. The weak toroidicity theory [8] predicts that CAEs are discrete eigenmodes and that for stronger toroidicity eigenmodes become more localized in poloidal angle near the equatorial plane on the Low Field Side (LFS). Thus, the previous theory that treats toroidicity perturbatively becomes invalid for large toroidicity such as in STs. This was also supported by our preliminary improved theory. Thus, we present in this section a new strong toroidicity theory for CAEs

and provide the CAE eigenmode structure and dispersion.

3.1 Equation for Compressional Alfvén Eigenmode.

We employ the cold plasma wave equation for the perturbed electric field in an inhomogeneous, magnetized plasma in toroidal geometry. The perturbed electric field satisfies Faraday's and Ampere's laws which reduce to the following equation:

$$\nabla \times \nabla \times \mathbf{E} = \frac{\omega^2}{c^2} \hat{\varepsilon} \cdot \mathbf{E}, \quad (1)$$

where $\hat{\varepsilon}$ is the dielectric permittivity tensor. We also assume vanishing parallel electric field, and the vector \mathbf{E} has two components perpendicular to the equilibrium magnetic field, and $\mathbf{E}(t) \sim \exp(-i\omega t)$. By neglecting the background ion and electron kinetic effects the cold plasma permeability tensor has the following tensor elements in the direction perpendicular to the magnetic field *only*

$$\hat{\varepsilon}_{11} = \hat{\varepsilon}_{22} = \sum_i \frac{\omega_{pi}^2}{\omega_{ci}^2 - \omega^2}, \quad (2)$$

$$\hat{\varepsilon}_{12} = -\hat{\varepsilon}_{21} = i \sum_i \frac{\omega}{\omega_{ci}} \frac{\omega_{pi}^2}{\omega_{ci}^2 - \omega^2}. \quad (3)$$

This is valid for oscillation frequency ω below the lower hybrid frequency. Here ω_{ci} and ω_{pi} are the ion cyclotron and ion plasma frequencies, respectively. Note that the dielectric tensor in Eq.(3) is rotationally invariant, which means that it can be used for any orthogonal coordinates perpendicular to the equilibrium magnetic field vector \mathbf{B} .

We will employ the Lagrange approach to find the solution of Eq.(3). Multiplying Eq.(1) by \mathbf{E}^* and integrating over the plasma volume we obtain the Lagrangian functional $\delta L = \int L d^3r$, where the Lagrangian density is

$$L = -|\nabla \times \mathbf{E}|^2 + \frac{\omega^2}{c^2} \mathbf{E}^* \cdot \hat{\varepsilon} \cdot \mathbf{E} = -k_{\parallel}^2 (|E_2|^2 + E_1^2) - (\mathbf{e}_2 \nabla E_1)^2 + \frac{\omega^2}{c^2} [\hat{\varepsilon}_{11} (E_1^2 + |E_2|^2) + \hat{\varepsilon}_{12} E_1 (E_2 - E_2^*)]. \quad (4)$$

Here we have chosen a local orthogonal system with the second component of the electric field along the direction of the wavevector $\mathbf{e}_2 \equiv \nabla E / |\nabla E|$, $E_2 = \nabla E^2 / 2|\nabla E|$, where E is the absolute value of the electric field. The

first component \mathbf{E}_1 is perpendicular to \mathbf{B} and \mathbf{e}_2 , and we define the operator $k_{\parallel} = \mathbf{b} \nabla \ln E$ where \mathbf{b} is the unit magnetic field vector. We also assume that E_1 is purely real and E_2 is purely imaginary (see below and Ref.[14]). Taking the variation of the Lagrangian functional with respect to the amplitude of second component of the electric field, we arrive at the equation determining the polarization of the compressional branch

$$E_2 = \frac{\hat{\epsilon}_{12}\omega^2/c^2}{-k_{\parallel}^2 + \hat{\epsilon}_{11}\omega^2/c^2} E_1 \equiv \frac{H}{F} E_1. \quad (5)$$

Note that by choosing this polarization we consider only the compressional Alfvén mode branch and do not consider the shear Alfvén branch. From Eq.(4) one can obtain the Lagrangian functional to determine the CAE eigenmode structure

$$\begin{aligned} \delta L &= \int \left[-(\nabla_{\perp} E_1)^2 + (F + H^2/F) E_1^2 \right] d^3 r = \\ &= \int \left[-(\nabla E_1)^2 + \left(\frac{\omega^2}{c^2} \hat{\epsilon}_{11} + H^2/F \right) E_1^2 \right] d^3 r. \end{aligned} \quad (6)$$

3.2 Eigenmode structure and dispersion.

In our previous theory we have neglected the contribution of $k_{\parallel}^2 \ll k_{\perp}^2$ in the mode structure [13]. However, for particle-wave interactions it is important to consider finite parallel wavevector, and we employ a WKB-ballooning representation for the poloidal angle dependence:

$$E = e^{-i\omega t + inq\theta - in\varphi} \sum_{j=-\infty}^{\infty} \hat{E}(r, \theta + 2\pi j) e^{i2\pi nqj} r / \sqrt{g^{11}} \sqrt{g} + c.c., \quad (7)$$

where the envelope function $\hat{E}(r, x^2)$ is nonperiodic and is required to be vanishing as $x^2 \rightarrow \pm\infty$. Here we dropped the subscripts for the electric field components, since all perturbed components are expected to be similar in their dependence on the spatial coordinates. Note that instead of the toroidal variable in Eq.(7) needs to be chosen in such a way that the magnetic field lines are straight. However one can show that this introduces a small correction to the dispersion hereafter if $q > 1$ at the mode location.

That the effective potential in Eq.(6) has a minimum near $x^2 = \theta = 0$ and at some $r = r_0$, which defines the mode localization. We define a curvilinear coordinate system as $x^1 = r$, $x^2 = \theta + 2\pi j$, and $x^3 = \varphi$. Metrics of such a

system is given by

$$\begin{aligned} g^{11} &= \kappa^{-2} \sin^2 x^2 + \cos^2 x^2, & g^{22} &= (x^1)^{-2} (\sin^2 x^2 + \kappa^{-2} \cos^2 x^2), \\ g^{12} = g^{21} &= -(1 - \kappa^{-2}) \sin x^2 \cos x^2, & g &= \kappa^2 (x^1)^2 R^2, \end{aligned} \quad (8)$$

where we retain finite ellipticity and the rest of the elements are $g^{13} = g^{31} = g^{23} = g^{32} = 0$. We then rewrite Lagrangian functional, Eq.(6), as

$$\begin{aligned} \delta L = & \int \left\{ \left(\hat{E} - \hat{E} \frac{\partial \ln(g^{11} \sqrt{g})}{2 \partial \ln x^1} + \frac{\partial \hat{E}}{\partial \ln x^1} \right)^2 + \frac{g^{22} (x^1)^2}{g^{11}} \left(-\hat{E} \frac{\partial \ln(g^{11} \sqrt{g})}{2 \partial x^2} + \frac{\partial \hat{E}}{\partial x^2} \right)^2 \right. \\ & + 2 \frac{g^{12} x^1}{g^{11}} \left(-\hat{E} \frac{\partial \ln(g^{11} \sqrt{g})}{2 \partial \ln x^1} + \frac{\partial \hat{E}}{\partial \ln x^1} \right) \left(-\hat{E} \frac{\partial \ln(g^{11} \sqrt{g})}{2 \partial x^2} + \frac{\partial \hat{E}}{\partial x^2} \right) \\ & \left. + (n x^1)^2 \left[(q' x^2)^2 + \frac{g^{22}}{g^{11}} (q)^2 + \frac{g^{33}}{g^{11}} + \frac{g^{12}}{g^{11}} 2 q q' x^2 + \frac{V(x^1, x^2)}{g^{11} (n x^1)^2} \right] \hat{E}^2 \right\} dx^1 dx^2, \end{aligned} \quad (9)$$

where $V(x^1, x^2) = (x^1)^2 \left(\frac{\omega^2}{c^2} \hat{\epsilon}_{11} + H^2/F \right)$, and the integration in x^2 is to be taken from $-\infty$ to ∞ . Note that the function V is periodic in poloidal angle, so that the solution is expected to have a wave-like behavior near its minima at $x^2 = 2\pi j$, and to decay exponentially from these wave-like regions. For small to medium n such a decaying behavior is important especially for the problem of CAE damping. Assuming that the coupling between j and $j + 1$ domains is small we will use a perturbation theory by introducing the coupling parameter $\eta \ll 1$.

3.2.1 CAEs Localized on LFS with $j = 0$.

First, we assume that the zeroth order CAE solution is localized at $x^2 = 0$ and the $j = 1$ domain is not coupled to the $j = -1$ domain. In this case we are looking for solutions in the form

$$\hat{E} \simeq \hat{E}_0 = e_0 \phi_m(\sqrt{2} x^2 / \Theta) \phi_s(\sqrt{2}(r - r_0) / \Delta), \quad (10)$$

where $\phi_s(x) = e^{-x^2/2} H_s(x) / \sqrt{n! 2^s \sqrt{\pi}}$ and H_s are the s -th order Chebyshev-Hermit functions and polynomials. Substituting this into Eq.(9), expanding coefficients near $\theta = 0$ and $r = r_0$, and integrating, we can make variations of the Lagrangian functional to obtain the required parameters Θ , Δ and the

CAE dispersion. The functional in this case is

$$\begin{aligned} \delta L_0/e_0 = & n^2 \left[\frac{q^2(r_0)}{\kappa^2} + \frac{R_0^2 + 4r_0^2}{4R_{00}^2} \right] + V_{00} + \left[n^2 D + \left(\frac{\partial^2 V}{2\partial r^2} \right)_{00} \right] \frac{\Delta^2}{2} \left(s + \frac{1}{2} \right) + \frac{s^2 + s + 3/2}{2} \\ & + \frac{(2s+1)r_0^2}{\Delta^2} + (n^2 T + V_{00} \tau) \frac{\Theta^2}{2} \left(m + \frac{1}{2} \right) + \frac{\kappa^4 - 1}{\kappa^4} \frac{m^2 + m + 3/2}{2} + \frac{2m+1}{\kappa^2 \Theta^2} - \frac{R_0^2}{4R_{00}^2} \end{aligned} \quad (11)$$

where T and D are given in the appendix, $\tau = \left(\partial^2 V / \partial (x^2)^2 / 2V \right)_{00} + 1 - \kappa^{-2}$, double zero subscript refers to the function evaluated at $x^2 = 0$ and $r = r_0$. Further analytical progress can be achieved with the assumption of $n \gg 1$. Also, we assume the following form for the safety factor $q = q_0(1 - \beta r^2/a^2)^{-\alpha}$, where $\beta = 1 - (q_0/q_a)^{1/\alpha}$, and q_a is the safety factor at the plasma edge. Note that the magnetic shear in this case is $s \equiv r q' / q = 2\alpha \beta r_0^2 / (a^2 - \beta r^2)$. To the lowest order in $1/nq$ the variation of the Lagrangian functional Eq.(11) with the respect to r_0 gives

$$\frac{r_0^2}{a^2} = \frac{\sigma + 1 + \beta(2\alpha' + 1) - \sqrt{[\sigma + 1 + \beta(2\alpha' - 1)]^2 + 8\beta\alpha'(\beta - 1)}}{2\beta(1 + \sigma + 2\alpha')}, \quad (12)$$

where we $\alpha' = \alpha n^2 q^2(r_0) / (n^2 q^2(r_0) + (\kappa^2 - 1)(m^2 + m + 3/2) / 2\kappa^2 + (2m + 1) / \Theta^2)$. For zero shear case, $\alpha = 0$, or for $m > nq(r_0)$ it reduces to $r_0^2/a^2 = 1/(1 + \sigma)$.

The variation with respect to Θ^2 yields

$$\Theta^2 = 2/\kappa \left(n^2 T + V_{00} \tau \right)^{1/2}. \quad (13)$$

From this equation we conclude that approximately $\Theta^2 = O\left((r_0 k_\perp)^{-1}\right)$. The condition for the poloidally localized CAE solution is $n^2 T - V_{00} \tau > 0$. The same procedure gives the following expression for the radial width

$$\Delta^2 = 2r_0 / \left(n^2 D + \left(\frac{\partial^2 V}{2\partial r^2} \right)_{00} \right)^{1/2}, \quad (14)$$

and $\Delta^2 = O(r_0/k_\perp)$. Comparing the last two equations one can conclude that the potential well for the eigenmode is shallow in poloidal direction and deep in radial. This implies that for the observed modes in NSTX we can consider $m \gg s$.

The dispersion of CAEs can be obtained by varying the Lagrangian with the respect to e_0 :

$$-V_{00} \simeq n^2 \left[\frac{q^2(r_0)}{\kappa^2} + \frac{R_0^2 + 4r_0^2}{4R_{00}^2} \right] + \frac{s^2 + s + 3/2}{2} + \frac{(4s+2)r_0^2}{\Delta^2} + \frac{\kappa^4 - 1}{\kappa^4} \frac{m^2 + m + 3/2}{2} + \frac{4m+2}{\kappa^2 \Theta^2} \quad (15)$$

In the limit of $\omega \ll \omega_{ci}$ and $\omega \gg \omega_{ci}$ as $V \simeq -r^2\omega^2/v_A^2$. Let us assume that the total magnetic field can be approximated as $B = B_0 R_0/R$. Such a magnetic field is formed in low to medium beta plasmas ($\beta_\varphi < 20\%$) in ST devices. Note that the effect of local diamagnetic magnetic well leads to a new type of CAEs and was considered in Ref.[15]. Thus, we obtain $\tau = -\epsilon + \alpha + 1 - \kappa^{-2}$. Using Eq.(13) to the lowest order in m we obtain from Eq.(15)

$$\Theta^2 \simeq \frac{-2}{\tau(m+1/2)} / \left(1 + \sqrt{-\tau^{-1} \left[\epsilon - \alpha + \frac{(\kappa - \kappa^{-1})^2}{2} + \frac{n^2}{(m+1/2)^2} \left(q^2 - \frac{\kappa^2 T}{\tau} \right) \right]} \right). \quad (16)$$

The equation for the radial width can be modified to the form

$$\Delta^2 \simeq 2r_0 \left(n^2 D + \left(\frac{4}{\tau \Theta^4 \kappa^2} - \frac{n^2 T}{\tau} \right) \left(\frac{\partial^2 V}{2V \partial r^2} \right)_{00} \right)^{-1/2}, \quad (17)$$

which together with Eqs.(15,16) determines the CAE dispersion relation.

Our choice of ballooning representation, Eq.(7), implies an estimate for parallel wavevector $k_{\parallel}^2 \simeq 4m/(qR\Theta)^2$. To derive analytical forms of the CAE dispersion we consider two cases $m < nq(r_0)$ and $m \simeq nq(r_0)$. In the first case $k \simeq (nq/r\kappa)_0$, and thus $k_{\parallel}/k_{\perp} \simeq (r_0/R_{00})^{5/4} \kappa \sqrt{m/nq(r_0)}/q(r_0)$. For the second case one obtains $k_{\parallel}/k_{\perp} \simeq (r_0/R_{00})^{5/4} \kappa/q(r_0)$. Note that the required large parallel wavevector for the observed sub-cyclotron instability should be relevant to the second case. Approximately in that case $k_{\parallel}/k_{\perp} \simeq (r_0/R_{00})^{5/4} \simeq 1/3$.

First we consider the case with $m < nq(r_0)$ with small k_{\parallel} . Since the Doppler shift to the cyclotron resonance is proportional to k_{\parallel} we expect that the CAE instability with such wavenumbers will be unstable at eigenfrequencies near the fast ion cyclotron frequency harmonics. Finally varying the Lagrangian functional with respect to the perturbed amplitude we obtain the CAE dispersion relation, which determines the CAE eigenfrequency at given quantum numbers m, s , and n ,

$$\begin{aligned} \omega_{0msn}^2 = & \frac{v_{A0}^2 n^2}{r_0^2} \left\{ \left[\frac{q^2}{\kappa^2} + \frac{R_0^2 + 4r_0^2}{4R_{00}^2} \right] + \left[D + \left(\frac{q^2}{\kappa^2} \frac{\partial^2 V}{2V \partial r^2} \right)_{00} \right]^{1/2} \frac{r_0(2S+1)}{n} + \frac{s^2 + s + 3/2}{2n^2} \right. \\ & \left. + \left(T - \frac{q^2 \tau}{\kappa^2} \right)^{1/2} \frac{2m+1}{kn} + \frac{\kappa^4 - 1}{\kappa^4} \frac{m^2 + m + 3/2}{2n^2} \right\}. \end{aligned} \quad (18)$$

Note that the condition for the poloidally localized CAE solution in this case is $T - \frac{q^2\tau}{\kappa^2} > 0$.

More relevant for the observed sub-ion cyclotron frequency CAEs is the case with $m > nq(r_0)$. To calculate the mode localization we assume $\epsilon > 1 - \kappa^{-2}$, which is valid especially in the localization region on the LFS of the plasma with finite triangularity. The variation of the Lagrangian functional with respect to the variable Θ , or Eq.(16), gives $\Theta^2 = 1/(\epsilon_0 - \alpha_0)(m + 1/2)$ to the lowest order in m , and

$$\begin{aligned} \omega_{0msn}^2 \simeq & \frac{v_{A00}^2}{r_0^2} \left\{ \frac{4(m+1/2)^2}{\kappa^2} (\epsilon_0 - \alpha_0) + \frac{\kappa^4 - 1}{\kappa^4} \frac{m^2 + m + 3/2}{2} \right. \\ & \left. + \frac{2(2s+1)(2m+1)}{\kappa} \sqrt{\frac{(\epsilon_0 - \alpha_0)(1+\sigma)}{2\sigma}} + n^2 \left[\frac{q^2(r_0)}{\kappa^2} + \frac{R_0^2 + 4r_0^2}{4R_{00}^2} \right] \right\}. \end{aligned} \quad (19)$$

where $\alpha_0 = B_\theta^2/2B_\varphi^2$ at $r = r_0$. The variation of the Lagrangian functional with respect to Δ results in $\Delta^2/r_0^2 = \kappa\sqrt{2\sigma/(1+\sigma)(\epsilon_0 - \alpha_0)}/(2m+1)$ and a correction to the mode eigenfrequency in Eq.(19).

3.2.2 CAEs Propagating to $j = \pm 1$.

To the zeroth order in η at each domain j the solutions are alike with the poloidal and radial mode structure described in the previous section. This can be verified by making corresponding variations of the Lagrangian. When the coupling is introduced the solution of the CAE should be

$$\hat{E} = \sum_{j=-1}^1 e_j \phi_m \left(\sqrt{2} (x^2 + 2\pi j) / \Theta \right) \phi_s \left(\sqrt{2} (r - r_0) / \Delta \right). \quad (20)$$

Substituting this form into the Eq.(9) we obtain a coupled system for the amplitudes e_j :

$$\begin{aligned} \delta L = & e_{-1}^2 \left[\delta(\omega_{msn}^2) + (nx^1 q')^2 (2\pi)^2 \right] + e_0^2 \delta(\omega_{msn}^2) \\ & + e_1^2 \left[\delta(\omega_{msn}^2) + (nx^1 q')^2 (2\pi)^2 \right] + (e_{-1}e_0 + e_1e_0) \left[\delta(\omega_{msn}^2) + (nx^1 q')^2 (\pi)^2 \eta \right], \end{aligned} \quad (21)$$

where the coupling parameter is $\eta = e^{-2\pi^2/\Theta^2} \Theta L_m(4\pi^2/\Theta^2)/\sqrt{2}$, L_m is m th order Laguerre polynomial, $\delta(\omega_{msn}^2)$ is the correction to the eigenfrequency. Making variations in e_j we obtain three coupled equations, which give $e_{-1} = e_1 = -e_0\eta/8$ and $\delta(\omega_{msn}^2) = -\eta/8$. In large m limit $\eta \rightarrow 0$. Figure 2 shows the η dependence on m , which shows that the coupling is weak. However

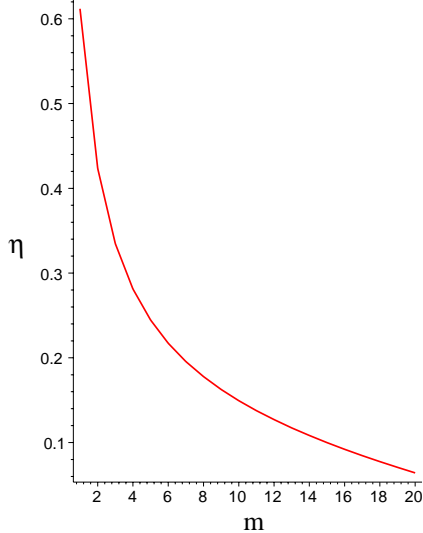


Figure 2: Coupling parameter η dependence on poloidal quantum wave number m .

the presence of $j = \pm 1$ harmonics may be noticeable near $\theta = \pi$. The eigenfrequency correction may be neglected, since $\delta(\omega_{msn}^2) = O(\omega_0^2 m^{-2}) \ll \omega_0^2$.

3.3 Estimates for observed spectra in NSTX.

Because accurate identification of CAE mode numbers has not been done experimentally yet, we will make an approximate comparison of the analytical CAE eigenfrequencies with the measured values. One of the explanation for the observed spectra of CAEs is given as follows. Different frequency peaks in each frequency band correspond to different m 's and are separated in frequency by (see Eq.(19))

$$\Delta f_m \simeq \frac{2v_A}{2\pi\kappa r} \sqrt{\epsilon_0 - \alpha_0}.$$

The large frequency separation $\Delta f \leq 1MHz$ seen between two bands of spectra peaks corresponds to a different radial wave numbers s , so that the frequencies are separated by

$$\Delta f_s \simeq \Delta f_m \kappa \sqrt{\frac{(1 + \sigma_i)}{2\sigma_i (\epsilon_0 - \alpha_0)}}.$$

For NSTX shot #103701 we use the following plasma parameters $B_{r=r_0} = 0.27T$, $r = 0.5m$, $\sigma_i = 0.5$, elongation $\kappa = 1.6$, $n_e = 2 \times 10^{13} cm^{-3}$. Also, the numerical equilibrium of this shot gives $\alpha_0 = 1/8$, with $\epsilon_0 = r_0/(R_0 + r_0) = 0.3$. We readily obtain $\Delta f_m = 150kHz$, and $\Delta f_s = 0.7MHz$. For #103431 with parameters $B_{r=r_0} = 0.32T$, $n_e = 4 \times 10^{13} cm^{-3}$, we obtain $\Delta f_m = 125kHz$, $\Delta f_s = 0.7MHz$. These results provide a reasonable quantitative agreement with the observed CAE spectra. Instability study should be done to understand the CAE excitation in ST.

4 Summary

A new theory of CAEs in axisymmetric low aspect ratio toroidal plasmas is developed and applied to interpret observations of new sub-ion cyclotron high frequency modes observed in NSTX. Based on the comparison between the observed magnetic fluctuation spectrum and the CAE theory we conclude that the observed modes in the frequency range from $f = 0.5MHz$ to $f = 2.5MHz$ are CAEs driven by fast super-Alfvénic NBI ions. A new finite aspect ratio CAE theory gives good agreement in frequency spacings between the m and $m + 1$ peaks as well as between the s and $s + 1$ CAE bands in the observed frequency spectrum. However, the stability study of CAEs due to fast beam ions is yet to be performed. We note that the ballooning formalism employed here to resolve CAE eigenstructure can also be employed to develop the instability theory because the ballooning formalism provides the expression of the parallel wavevector as a function in the real space.

A Coefficients T and D .

Straightforwardly one obtains the coefficients for the CAE problem from the Lagrangian Eq.(11):

$$\begin{aligned}
 T = & \left(1 - \frac{1}{\kappa^4}\right) q(r_0)^2 + r_0^2 \left(\frac{\partial q}{\partial r}\right)_0^2 - 2r_0 \left(1 - \frac{1}{\kappa^2}\right) \left(q \frac{\partial q}{\partial r}\right)_0 + \frac{R_0^2 r_0}{4R_{00}^3} \\
 & + \frac{1}{\kappa^2} \left(1 - \frac{1}{\kappa^2} + \frac{r_0}{2R_{00}}\right)^2 - \frac{R_0}{R_{00}} \left(1 - \frac{1}{\kappa^2}\right) \left(1 - \frac{1}{\kappa^2} + \frac{r_0}{2R_{00}}\right) + \frac{r_0^2}{R_{00}^2} \left(1 - \frac{1}{\kappa^2} + \frac{r_0}{R_{00}}\right)
 \end{aligned}
 \tag{22}$$

$$D = \frac{1}{\kappa^2} \left(\frac{\partial q}{\partial r}\right)_0^2 + \left(\frac{q}{\kappa^2} \frac{\partial^2 q}{\partial r^2}\right)_0 + \frac{R_0^2}{R_{00}^3 r_0}.$$

References

- [1] GREENE, G. J., *et al.*, in *Proceedings of 17th European Conference on Controlled Fusion and Plasma Heating*, Amsterdam, Netherlands, 1990, edited by G. Briffod, Adri Nijssen-Vis, and F. C. Schüller (European Physical Society, Petit-Lancy, Switzerland, 1990), Part IV, Vol. 14B, p.1540.
- [2] COTTRELL, G. A., DENDY, R. O., *Phys. Rev. Lett.* **60** (1988) 33 .
- [3] COTTRELL, G. A., *et al.*, *Nucl. Fusion* **33** (1993) 1365.
- [4] S. CAUFFMAN, R. MAJESKI, K. G. McCLEMENTS, *et al.*, *Nucl.Fusion*, **35** (1995) 1597.
- [5] S. M. KAYE, M. ONO, Y-K. M. PENG, *et.al.* *Fusion Technology* **36** 16 (1999).
- [6] Y-K. M. PENG, *Phys. Plasmas* **7** 1681 (2000) 1681.
- [7] E. FREDRICKSON, *et al.*, to appear in PRL 2001.
- [8] N. N. GORELENKOV, C. Z. CHENG, *Nucl. Fusion* **35** (1995) 1743.
- [9] T. FŮLŮP, Ya. KOLESNICHENKO, M. LISAK, *et al.*, *Nucl. Fusion* **37** (1997) 1281.
- [10] T. FŮLŮP, M. LISAK, *Nucl. Fusion* **38** (1998) 761.
- [11] S. M. MAHAJAN, ROSS, D. W., *Phys. Fluids* **26** (1983) 2561.
- [12] B. COPPI, *et.al.*, *Phys. Fluids* **29** (1986) 4060.
- [13] N. N. GORELENKOV, C. Z. CHENG, *et al.*, submitted to *Nucl. Fusion*.
- [14] AKHIEZER, A. I., *et al.*, *Plasma Electrodynamics* (Pergamon Press, Oxford, New York, 1975), Vol.1.
- [15] M. V. GORELENKOVA, N. N. GORELENKOV, *Phys. Plasmas* **5** (1998) 4104.
- [16] N. N. GORELENKOV, C. Z. CHENG, *Phys. Plasmas* **2** (1995) 1961.

External Distribution

Plasma Research Laboratory, Australian National University, Australia
Professor I.R. Jones, Flinders University, Australia
Professor João Canalle, Instituto de Fisica DEQ/IF - UERJ, Brazil
Mr. Gerson O. Ludwig, Instituto Nacional de Pesquisas, Brazil
Dr. P.H. Sakanaka, Instituto Fisica, Brazil
The Librarian, Culham Laboratory, England
Library, R61, Rutherford Appleton Laboratory, England
Mrs. S.A. Hutchinson, JET Library, England
Professor M.N. Bussac, Ecole Polytechnique, France
Librarian, Max-Planck-Institut für Plasmaphysik, Germany
Jolan Moldvai, Reports Library, MTA KFKI-ATKI, Hungary
Dr. P. Kaw, Institute for Plasma Research, India
Ms. P.J. Pathak, Librarian, Institute for Plasma Research, India
Ms. Clelia De Palo, Associazione EURATOM-ENEA, Italy
Dr. G. Grosso, Instituto di Fisica del Plasma, Italy
Librarian, Naka Fusion Research Establishment, JAERI, Japan
Library, Plasma Physics Laboratory, Kyoto University, Japan
Research Information Center, National Institute for Fusion Science, Japan
Dr. O. Mitarai, Kyushu Tokai University, Japan
Library, Academia Sinica, Institute of Plasma Physics, People's Republic of China
Shih-Tung Tsai, Institute of Physics, Chinese Academy of Sciences, People's Republic of China
Dr. S. Mirnov, TRINITI, Troitsk, Russian Federation, Russia
Dr. V.S. Strelkov, Kurchatov Institute, Russian Federation, Russia
Professor Peter Lukac, Katedra Fyziky Plazmy MFF UK, Mlynska dolina F-2, Komenskeho
Univerzita, SK-842 15 Bratislava, Slovakia
Dr. G.S. Lee, Korea Basic Science Institute, South Korea
Mr. Dennis Bruggink, Fusion Library, University of Wisconsin, USA
Institute for Plasma Research, University of Maryland, USA
Librarian, Fusion Energy Division, Oak Ridge National Laboratory, USA
Librarian, Institute of Fusion Studies, University of Texas, USA
Librarian, Magnetic Fusion Program, Lawrence Livermore National Laboratory, USA
Library, General Atomics, USA
Plasma Physics Group, Fusion Energy Research Program, University of California at San
Diego, USA
Plasma Physics Library, Columbia University, USA
Alkesh Punjabi, Center for Fusion Research and Training, Hampton University, USA
Dr. W.M. Stacey, Fusion Research Center, Georgia Institute of Technology, USA
Dr. John Willis, U.S. Department of Energy, Office of Fusion Energy Sciences, USA
Mr. Paul H. Wright, Indianapolis, Indiana, USA

The Princeton Plasma Physics Laboratory is operated
by Princeton University under contract
with the U.S. Department of Energy.

Information Services
Princeton Plasma Physics Laboratory
P.O. Box 451
Princeton, NJ 08543

Phone: 609-243-2750
Fax: 609-243-2751
e-mail: pppl_info@pppl.gov
Internet Address: <http://www.pppl.gov>